PHYSICAL REVIEW E **89**, 050301(R) (2014)

Molecular dynamics simulation of short-wavelength collective dynamics of phospholipid membranes

Valeria Conti Nibali,[1] Giovanna D'Angelo,[1,*] and Mounir Tarek[2,†]
[1]*Dipartimento di Fisica, Università degli Studi di Messina, Messina, Italy*
[2]*UMR Structure et Réactivité des Systèmes Moléculaires Complexes, Nancy University, CNRS, Nancy, France*
(Received 3 February 2013; published 12 May 2014)

We investigated the short-wavelength longitudinal and transverse collective dynamics of the fluid and gel phases of phospholipid bilayers by means of molecular dynamics simulation. Similarly to a crystal, the spectrum of collective excitations in a bilayer consists of longitudinal and transverse acoustic modes, though modified by disorder. Beside acoustic modes, a series of broad dispersionless excitations are revealed. The dispersion curves of the observed excitations may be represented in a pseudo-Brillouin zone scheme centered around the spatial correlation peak of the acyl chains. The study provides evidence for a resonant interaction between the lowest frequency optical phonon and the longitudinal acoustic mode.

DOI: 10.1103/PhysRevE.89.050301 PACS number(s): 83.10.Mj, 87.14.Cc, 83.85.Hf, 87.16.dj

The study of dynamical processes in phospholipid bilayers as models of natural membranes has constituted a very active field of research during the past two decades. Short-wavelength collective dynamics of lipid bilayers investigated by means of inelastic x-ray (IXS) [1] and neutron (INS) scattering experiments [2] and molecular dynamics (MD) simulations [3–5] indicate the existence of a well-defined acousticlike excitation attributed to the in-plane motions of the hydrocarbon chains. This excitation shows a linear increase at the small in-plane wave vector Q due to long-wavelength sound propagation, saturating at some maximum value at $Q_{\max/2}$. At higher Q, a pronounced minimum is observed at $Q_{\max} = 1.4$ Å^{-1}, corresponding to the nearest-neighbour distances of lipid acyl tails and to the maximum of the static structure factor $S(Q)$. $Q_{\max}$ has been interpreted as the pseudo-Brillouin zone of a two-dimensional liquid [2]. The dispersion of the revealed excitation has been considered as indicative of a simple-liquid behavior and described in the theoretical framework of hydrodynamics [6]. However, despite the success of this approach in predicting the thermal and elastic constants in the hydrodynamic limit, several findings suggest that the collective dynamics of lipid bilayers strongly differs from that outlined for simple liquids. Among these evidences are the linear (instead of quadratic) momentum transfer Q dependence of the width of the Brillouin lines [6] and the existence of an opticlike mode found at 14 meV in the gel phase and at 7 meV in the liquid crystal phase [2,3].

Actually, lipid bilayers are complex viscous fluids in which propagating shear waves and opticlike modes arising from mass-concentration fluctuations are expected to emerge even in the hydrodynamic region. Propagating transverse motions are still unexplored despite their influence on the elasticity of lipid bilayers [7] and in transmembrane transport of small molecules [8], and only scarce information is available on opticlike excitations. On the other hand, lipid bilayers, as do smectic liquid crystals, show elements of order that should contrast the effect of thermal fluctuations, favoring the propagation of collective motions on an extended Q range. In order to thoroughly address these issues, we present here MD simulation analyses of the coherent collective longitudinal and transverse motions of model membranes in the THz frequency regime. We show the existence of longitudinal and transverse acousticlike and opticlike modes whose dispersion curves may be represented in a pseudo-Brillouin zone scheme centered around $Q_{\max}$, thus reminding one of the lattice dynamics of a crystal.

Differently from the previous works focusing on the dynamical structure factor $S(Q,E)$ [1–4], our analysis is based on the direct investigation of the longitudinal $C_L(Q,E)$ and transverse $C_T(Q,E)$ current correlation spectra (see Supplemental Material [9]). We have calculated the time correlation functions $C_\alpha(\boldsymbol{Q},t) = \langle \mathbf{J}^*_\alpha(\boldsymbol{Q},t) \cdot \mathbf{J}_\alpha(\boldsymbol{Q},t) \rangle$ of the longitudinal ($\alpha = L$) and the transverse ($\alpha = T$) currents determined at a wave vector $\boldsymbol{Q}$ and defined respectively as $\mathbf{J}_L(\boldsymbol{Q},t) = N^{-1/2} \sum_i \hat{\boldsymbol{Q}}[\hat{\boldsymbol{Q}} \cdot \mathbf{v}_i(t)] \exp[-j\,\boldsymbol{Q} \cdot \mathbf{r}_i(t)]$ and $\mathbf{J}_T(\boldsymbol{Q},t) = N^{-1/2} \sum_i \hat{\boldsymbol{Q}} \times \mathbf{v}_i(t) \exp[-j\,\boldsymbol{Q} \cdot \mathbf{r}_i(t)]$, where $\hat{\boldsymbol{Q}}$ is the unit vector along $\boldsymbol{Q}$, $\mathbf{r}_i(t)$ and $\mathbf{v}_i(t)$ are the positions and velocities of atom i, and N is the total number of atoms. $C_L(Q,E)$, the time Fourier transform of $C_L(Q,t)$, is also directly coupled to the dynamics of the collective density fluctuations in the system and to $S(Q,E)$, by means of $C_L(Q,E) = E^2 S(Q,E)/Q^2$. In contrast, $C_T(Q,E)$ probes the shear modes possibly propagating in the system at a given wave vector. It is worth noting that the collective modes describing density fluctuations are hardly observable in the dynamics structure factor $S(Q,E)$, where they appear as weak shoulders in the tails of the elastic peak at the lowest Q, while they tend to be buried in the spectrum at higher Q due to their increasing damping. Conversely, in $C_L(Q,E)$, due to the presence of the E^2 factor, the elastic peak that dominates the $S(Q,E)$ is effectively suppressed, while the contribution of the modes at higher frequencies is emphasized [10]. Collective modes appear as peaks in the $C_\alpha(Q,E)$ spectra, and their nature can be determined by knowing their frequency change as a function of Q. The membrane models considered here are fully hydrated dimyristoyl-phosphatidylcholine (DMPC) lipid bilayers. We investigated both the liquid crystal (hereafter referred to as liquid) phase (at 303 K, i.e., 6 K above T_m, the gel to liquid transition temperature) and the gel phase (at 283 K, i.e., 15 K below T_m [11]). The initial configurations were taken from previous investigations [3] and replicated

*gdangelo@unime.it
†mtarek@uhp-nancy.fr

in order to generate large systems containing 384 lipids hydrated with 25.7 water molecules/lipid for the liquid phase, and 256 lipids hydrated with 11.8 water molecules/lipid for the gel phase. The MD simulations were carried out using NAMD2 [12]. The two systems were first equilibrated at constant temperature and constant pressure (1 atm) using three-dimensional (3D) periodic boundary conditions and employing a Langevin dynamics and Langevin piston method. Long-range electrostatic forces were taken into account using the particle mesh Ewald approach [13]. The water molecules were described using the TIP3P model. The all-atom force field parameters for the lipid were extracted from CHARMM27 [14] and modified according to the recommendations by Hogberg *et al.* [15]. Following over 30 ns MD simulations for each system performed at constant pressure, 200 ps runs were performed at constant volume, and the atomic positions and velocities, saved every fs, were collected for the analyses of the correlation functions. Here we focus on the lipid dynamics by monitoring the motions of hydrocarbon chain C atoms [16]. Accordingly, the correlation functions were calculated for each given $Q = |Q|$, with the value Q lying in the plane of the bilayer [17]. The $C_\alpha(Q,E)$ current spectra of the DMPC gel and liquid phases computed from the simulations are reported in Fig. 1. Despite the considerable differences in the structure and densities, the two phases present similar characteristics: At low Q values (<0.8 Å^{-1}), both longitudinal and transverse spectra show a distinct excitation with a dispersive character. Importantly, in contrast with hydrodynamics that predicts that transverse fluctuations are transported diffusively and contribute to the spectrum only with a peak at $E = 0$, the presence of a well-defined peak at $E \neq 0$ also in $C_T(Q,E)$ proves that lipid membranes can support long-wave transverse acousticlike excitations in both liquid and gel phases. At higher Q, the spectra atypically broaden out and additional excitations are observed. Since these latter are more clearly visible in the gel phase due to a reduced molecular mobility with respect to the liquid phase, henceforward we focus on the DMPC gel. Furthermore, although these excitations are observable in $C_\alpha(Q,E)$ at relatively high Q values, it is conceivable that they are hidden under the intense main propagating excitation at low Q values. Thus we assume that they have to be taken into account over the entire investigated Q range for a full description of the lipid dynamics. In order to estimate the number of excitations that characterize lipid dynamics, we have examined the $C_\alpha(Q,E)$ spectra of the gel phase around $Q_{\max}$.

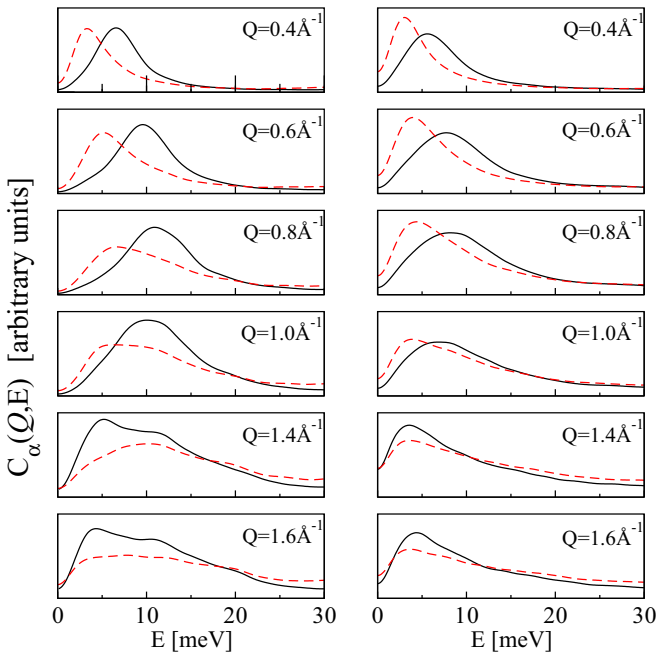

FIG. 1. (Color online) Longitudinal (solid black) and transverse (dashed red) current spectra $C_\alpha(Q,E)$ of the DMPC gel (left) and liquid (right) phase at selected Q values ranging from 0.4 to 1.6 Å^{-1}. The current spectra were generated from the Fourier transform of the product of $C_\alpha(Q,t)$ with a Gaussian window function in order to reduce the noise in the Fourier transform.

All the excitations have been described by damped harmonic oscillator (DHO) functions [18] and taken into account in the fitting procedure of the $C_\alpha(Q,E)$ spectra, which can thus be expressed as $C_\alpha(Q,E) = \sum_i \mathrm{DHO}_i \times E^2 = \sum_i [A_i(Q)\Gamma_i(Q)E_i^2(Q)E^2]/\{[E^2 - E_i^2(Q)]^2 + [\Gamma_i(Q)E]^2\}$, where $\Gamma_i(Q)$ is the energy width (damping coefficient), $E_i(Q)$ the average excitation energy, and $A_i(Q)$ the amplitude of the inelastic signal. In this way, as shown in Figs. 2(a) and 2(b), we were able to resolve a total of six excitations in both $C_T(Q,E)$ and $C_L(Q,E)$ at $E < 25$ meV (see the Supplemental Material [9]). Figure 2(c) shows the dispersion curves determined by fitting the $C_\alpha(Q,E)$ in the studied Q range. In both $C_L(Q,E)$ (open symbols) and $C_T(Q,E)$ (solid symbols) spectra we identify two acousticlike modes and four opticlike excitations, having similar frequencies. These findings indicate that all the revealed modes have a mixed (longitudinal and transverse) symmetry character. Notably, at low Q the main component of $C_T(Q,E)$ is the acoustic mode of lower energy (red) while the main component of $C_L(Q,E)$ is the acoustic mode of higher energy (black). We assign therefore the former to a quasitransverse acoustic branch (hereafter referred to as the TA mode) and the latter to a quasilongitudinal acoustic branch (hereafter referred to as the LA mode).

The mixed symmetry character probably stems from the lack of translational invariance in the investigated systems, analogously to what has been found [19,20] in other disordered systems. Interestingly, the dispersion relations for both transverse and longitudinal modes derived here show a minimum near $Q_{\max}$, the wave vector at which the static structure factor $S(Q)$ of the membrane has its first maximum (inter-acyl-chain correlation peak). This minimum arises from a process analogous to the umklapp scattering in crystalline solids: The sharp first maximum in the static structure factor acts as a smeared-out reciprocal-lattice vector, i.e., a pseudo-Bragg peak. Furthermore, as in a periodic crystal, (i) the TA and LA acoustic branches are symmetric around the $\frac{Q_{\max}}{2}$ point in reciprocal space, thus defining the boundary of a pseudo-Brillouin-zone (Q_{PBZ}); (ii) in correspondence to the energy at which the LA branch crosses the first and second pseudo-Brillouin zones ($E \approx 10$ meV), a pseudogap opens and an opticlike branch (12 meV) near Q_{PBZ} is observed; and (iii) the intensity of the LA and TA phonons [shown in Fig. 3(c)] is modulated by that of the pseudo-Bragg peak. However, in

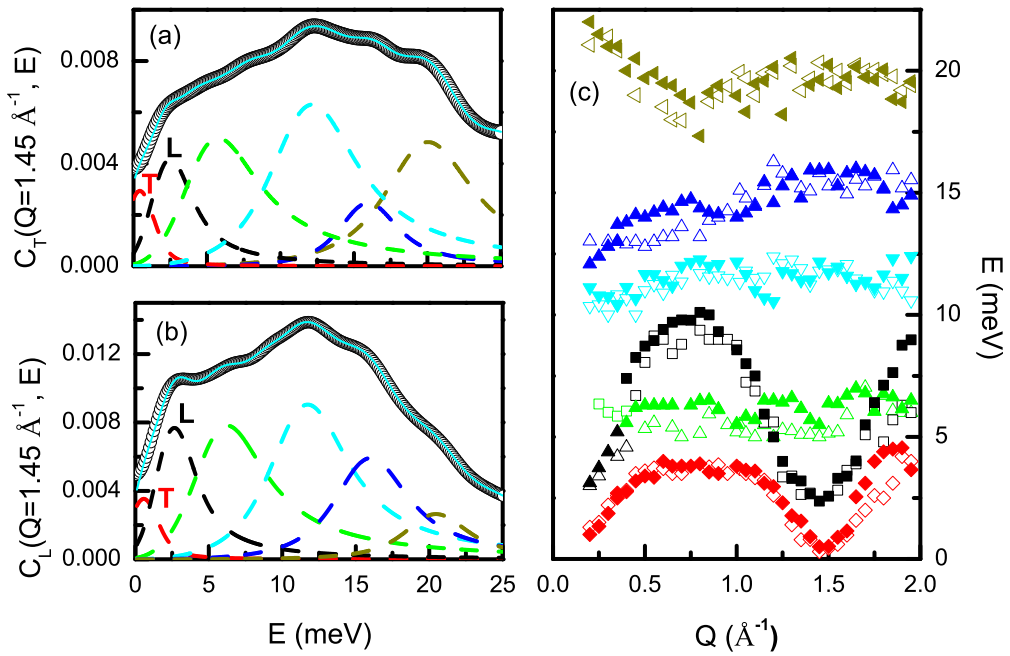

FIG. 2. (Color online) (a) Transverse and (b) longitudinal current spectra for the DMPC gel phase calculated at $Q = 1.45$ Å^{-1} (symbol) and their fit (solid line) with six components (dashed lines). (c) Full dispersion curves of the six components of the longitudinal (solid symbols) and transverse (open symbols) current spectra of the DMPC gel phase.

contrast to the crystalline state, all the collective excitations have a finite lifetime. In fact, the damping of all modes is $\neq 0$ in the whole Q range [Fig. 3(c)]. In particular, for LA and TA modes, the damping increases up to Q_{PBZ}, showing a linear growth up to $Q = 0.4$ Å^{-1}. Then it decreases to a minimum at Q_{max}, since the strong spatial correlations of the acyl chains at $2\pi/Q_{max}$ favor propagation of the acousticlike modes. Quite curiously, the propagation of the LA mode is strongly perturbed in the range of 4–8 meV, where the lowest frequency dispersionless branch (i.e., opticlike) at $\simeq$6 meV

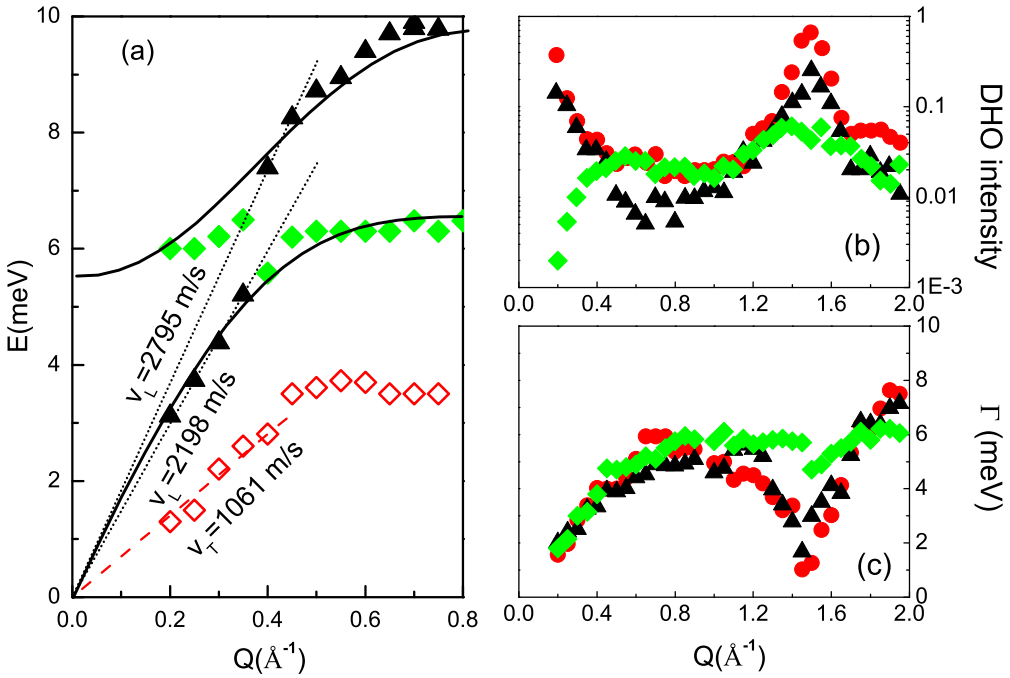

FIG. 3. (Color online) (a) Low energy phonon dispersion curve illustrating the symmetry avoided crossing between the LA mode (black triangles) with the localized vibration (green diamonds) (see text for details). The two black dotted lines correspond to the fast and normal sound branches. Red open diamonds and the red dashed line represent the TA branch and the linear fit for $Q < 0.4$ Å^{-1}, respectively; (b) and (c) show respectively the DHO integrated area and DHO width for the LA mode (black triangles), TA mode (red circles), and optical mode at 6 meV (green diamonds).

is observed (see Fig. 3). In particular, in the hydrodynamic region ($Q < 0.4$ Å^{-1}), the dispersion relation of the LA mode is linear with a sound velocity $v_L \simeq 2198$ m s^{-1}, in good agreement with the value (2230 m s^{-1}) reported from IXS experiments for the gel phase of DMPC [1]. Differently, above $Q = 0.4$ Å^{-1}, v_L increases to 2795 m s^{-1} (27%). This observed fast sound, together with the energy matching between the dispersionless branch at $\simeq$6 meV and the LA mode, suggest the existence of a symmetry avoided crossing [21,22] that leads to the change in v_L. An avoided crossing leads to a coupling between a localized excitation and an acoustic vibration with a consequent energy exchange from the dispersive mode to the nondispersive one. Before the crossing event, the nondispersive mode behaves as an independent oscillator and is characterized by a very small (negligible) intensity compared to the one of the dispersive mode. At $Q_{\text{anticross}}$ a transfer of the intensity from the acoustic phonon to the nondispersive mode occurs and, consequently, the latter becomes visible in the spectra. Within this framework the opticlike mode at 6 meV appears to anticross the LA mode at $Q_{\text{anticross}} = 0.4$ Å^{-1} [Fig. 3(a)]. As confirmation of this assumption in Fig. 3(b), the intensities (DHO integrated areas) of the two modes involved in the process are shown: At $Q_{\text{anticross}}$, we observe a clear reversal in the corresponding mode intensities.

As for the TA mode, we observe an initial increase of the excitation energy with increasing Q with velocity $v_T = 1061$ m s^{-1}. Moreover, we note the in the proximity of $Q_{\max}$ the intensity of the TA mode visibly increases, exceeding that of the LA mode [see Fig. 3(c)]. Concerning the optical modes, the one at $\simeq$6 meV can be tentatively attributed to terminal carbon dynamics, as posited in previous simulations [3] and experiments [2], while the modes at $\simeq$12, 15, and 20 meV could originate from an intermolecular hydrogen-bonding structure and or from the molecular breathing within the bilayer as, suggested by recent far-IR studies [23]. The analysis presented here is a prerequisite to appropriately understand raw data from the experiments. Accurate experimental investigations have to be performed to confirm this scenario and to ascertain the existence of the revealed excitations. In principle, owing to their mixed symmetry character, all the modes can be probed by INS or IXS experiments that monitor $S(Q,E)$. Interestingly, the data at hand suggest that such experiments could probe the transverse dynamics (TA mode) by looking at the quasitransverse branch of the longitudinal current spectra close to the strong Bragg peak at $Q_{\max}$ (black solid symbols in Fig. 3). If the LA and TA excitations are not well separated, inelastic scattering techniques will mainly probe the modes with the highest intensities, which may result in misattribution. This is precisely what seems to be the case for earlier investigations [1–3,5] that have revealed just one excitation for $E < 12$ meV. In Fig. 4 we have compared our data for the DMPC gel phase to those reported by others.

At low momentum transfer ($Q < 0.5$ Å^{-1}) the mode identified by all previous studies [1,3,5] coincides quite well with the LA mode. At higher momentum transfers, and in particular in the vicinity of $Q_{\max}$, the excitation energy determined by the high energy resolution INS [2] and MD [3] departs from that of the herein identified LA mode and coincides more with the TA mode. This suggests that around $Q_{\max}$ these techniques have mainly probed the highest intensity (TA) mode [see Fig. 3(c)]. Finally, we note that a second excitation revealed (around $Q_{\max}$) by INS (see Fig. 4) has been interpreted as traces of the "fluid excitation" due to the coexistence of fluid and gel domains [2]. Interestingly, its energy is very close to that of the LA mode of the pure gel phase investigated by the present simulation, suggesting that INS could have probed both the intense TA and LA modes around $Q_{\max}$. This issue could be clarified by further experiments probing a pure gel phase, i.e., without fluid domains.

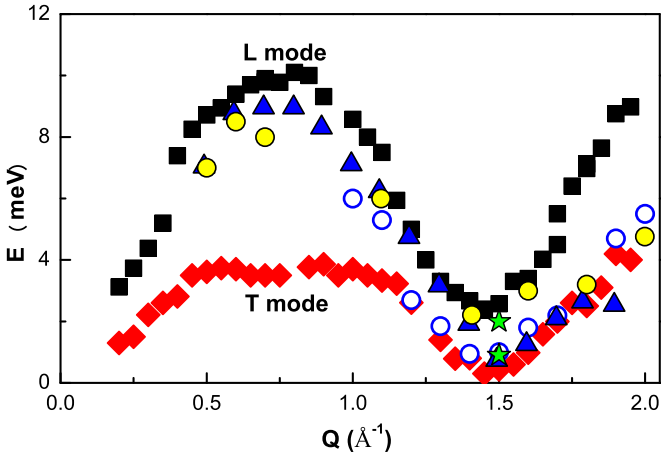

FIG. 4. (Color online) Dispersion curves of the LA (black squares) and TA (red diamonds) modes from $C_L(Q,E)$ of the DMPC gel phase from the present simulations and from previous investigations: Ref. [3] (blue triangles), Ref. [2] (blue open circles), and Ref. [1] (yellow solid circles). Green stars indicate the energies of the two modes revealed by INS at $Q = 1.5$ Å^{-1} [2].

In summary, the analyses performed here have allowed us to uncover a different scenario for the interpretation of the short-wavelength collective dynamics of phospholipid bilayers. The study revealed (i) propagating long-wave acousticlike transverse modes, and (ii) acousticlike and opticlike modes with mixed symmetry character. This challenges the oversimplified interpretations of collective motions in membranes in terms of simple liquids. Some observed excitations predicted by simulations await experimental verification, and much work is needed to understand the incidence of such dynamics in complex biomembranes. We believe, however, that studies along the lines of the investigations performed here will likely enhance our understanding of such materials.

V.C.N. has carried out research under an HPC-EUROPA2 project. Calculations were performed at the CINES supercomputer center (Montpellier, France). The authors are grateful to Salvatore Patané for help with data fitting.

[1] S. H. Chen *et al.*, Phys. Rev. Lett. **86**, 740 (2001).

[2] M. C. Rheinstädter, C. Ollinger, G. Fragneto, F. Demmel, and T. Salditt, Phys. Rev. Lett. **93**, 108107 (2004).

[3] M. Tarek, D. J. Tobias, S. H. Chen, and M. L. Klein, Phys. Rev. Lett. **87**, 238101 (2001).

[4] J. S. Hub, T. Salditt, M. C. Rheinstader, and B. L. de Groot, Biophys. J. **93**, 3156 (2007).
[5] E. G. Brandt and O. Edholm, Biophys. J. **96**, 1828 (2009).
[6] J. P. Boon and S. Yip, *Molecular Hydrodynamics* (McGraw-Hill, New York, 1980).
[7] G. Espinosa, I. Lopez-Montero, F. Monroya, and D. Langevin, Proc. Natl. Acad. Sci. USA **108**, 6008 (2011).
[8] M. D. Kaye, K. Schmalzl, V. C. Nibali, M. Tarek, and M. C. Rheinstädter, Phys. Rev. E **83**, 050907(R) (2011).
[9] See Supplemental Material at http://link.aps.org/supplemental/10.1103/PhysRevE.89.050301 for a detailed description of the fitting procedure.
[10] V. Conti Nibali, G. D'Angelo, A. Paciaroni, D. J. Tobias, and M. Tarek, J. Phys. Chem. Lett. **5**, 1181 (2014).
[11] G. D'Angelo, U. Wanderlingh, V. Conti Nibali *et al.*, Philos. Mag. **88**, 4033 (2008).
[12] J. C. Phillips *et al.*, J. Comput. Chem. **26**, 1781 (2005).
[13] U. Essmann, L. Perera, M. L. Berkowitz, T. Darden *et al.*, J. Chem. Phys. **103**, 8577 (1995).
[14] S. E. Feller, D. Yin, R. W. Pastor, and A. D. MacKerell, Jr., Biophys. J. **73**, 2269 (1997).
[15] C. J. Hogberg, A. M. Nikitin, and A. P. Lyubartsev, J. Comput. Chem. **29**, 2359 (2008).
[16] Carbons of the methyl groups have been excluded from this analysis since their dynamical behavior has been previously studied [3].
[17] In the simulation, $\boldsymbol{Q}$ are restricted to $\boldsymbol{Q} = l\mathbf{a}_i^* + m\mathbf{a}_j^*$, where l and m are integers and $\mathbf{a}_i^*$ and $\mathbf{a}_j^*$ the in-plane reciprocal lattice vectors of the simulation cell. The values of $Q = |\boldsymbol{Q}|$ were chosen between 0.2 and 2.00 Å^{-1} at 0.05 Å^{-1} intervals, and the number of contributing vectors (l,m values) to each Q varied from 15 to 35.
[18] D. Liu *et al.*, Phys. Rev. Lett. **101**, 135501 (2008).
[19] M. Sampoli, G. Ruocco, and F. Sette, Phys. Rev. Lett. **79**, 1678 (1997).
[20] O. Pilla, S. Caponi, A. Fontana, J. R. Concalves *et al.*, J. Phys.: Condens. Matter **16**, 8519 (2004).
[21] J. von Neumann and E. Wigner, Phys. Z. **30**, 467 (1929).
[22] J. Baumert, C. Gutt, V. P. Shpakov, J. S. Tse *et al.*, Phys. Rev. B **68**, 174301 (2003).
[23] R. Hielscher and P. Hellwig, ChemPhysChem **11**, 435 (2010).